Journal of Neonatal Surgery
ISSN (Online): 2226 -0439
Vol. 14, Issue 32s (2025)
https://www.jneonatalsurg.com

OPEN ACCESS

In-silico & In-Vitro study for Assessment of Antimicrobial and Antioxidant activity of the secondary metabolites containing the leaves extract of *Acacia suma* L.

Dr. Nilip Kanti Deb [1], Soumi Chattopadhyay[2], Anusree Raha[3], Prosenjit Mukherjee[4], Monit Pal[5], Palash Chandra Biswas[6], Anindya Bagchi [7*]

[1]Principal, Professor, Vidyasagar Pharmaceutical College of Education, Simurali, Nadia, West Bengal.

Email ID: nilipkdeb@gmail.com

[2]Assistant Professor, Pharmaceutical Chemistry, Vidyasagar Pharmaceutical College of Education, Simurali, Nadia, West Bengal.

Email ID: souminh99@gmail.com

[3]Associate Professor, Pharmaceutics, Netaji Subhas Chandra Bose Institute of Pharmacy, Chakdaha, West Bengal, India. Makaut.

Email ID: glassheaven111@gmail.com

[4]Associate Professor, Pharmaceutical Chemistry, Netaji Subhas Chandra Bose Institute of Pharmacy, Chakdaha, West Bengal, India. Makaut.

Email ID: prosen.pharmchem@gmail.com

[5]Associate Professor, Pharmaceutical Chemistry, Netaji Subhas Chandra Bose Institute of Pharmacy, Chakdaha, West Bengal, India. Makaut,

Email ID: monitpl1@gmail.com

[6]Assistant Professor, Pharmaceutical Chemistry, Netaji Subhas Chandra Bose Institute of Pharmacy, Chakdaha, West Bengal, India. Makaut,

Email ID: palashbiswas76@yahoo.com

[7*]Associate Professor, Pharmaceutical Chemistry, Netaji Subhas Chandra Bose Institute of Pharmacy, Chakdaha, West Bengal, India. Makaut,

Email ID: tajuanindya@gmail.com

***Corresponding Author:**

Anindya Bagchi

*Associate Professor, Pharmaceutical Chemistry, Netaji Subhas Chandra Bose Institute of Pharmacy, Chakdaha, West Bengal, India. Makaut,

Email ID: tajuanindya@gmail.com

Cite this paper as: Dr. Nilip Kanti Deb , Soumi Chattopadhyay, Anusree Raha, Prosenjit Mukherjee, Monit Pal, Palash Chandra Biswas, Anindya Bagchi, (2025) *In-silico* & In-Vitro study for Assessment of Antimicrobial and Antioxidant activity of the secondary metabolites containing the leaves extract of *Acacia suma* L.. *Journal of Neonatal Surgery*, 14 (32s), 218-242.

ABSTRACT

One of the main sources for developing new, efficient medications is thought to be medicinal plants. In this context, the study's objectives were to determine whether polyphenolic and flavonoid fractions were present using phytochemical screening in chloroform extracts of ***Acacia suma L*** leaves and to assess the antibacterial and antioxidant properties of these fractions. Additionally, *in silico* analysis was carried out using the extract's phytochemical screening as a basis, and it was followed by previously reported compounds with antibacterial activity contributed by phenolic, terpenoids, and flavonoids—present in the plant extract as it was confirmed by LC-MS/MS results of the extract obtained during the study. The principle behind this analysis is molecular docking, which uses PyRx software to predict activity, and the Swiss ADME web portal was used to perform ADME analysis of the same reported phytoconstituents in order to infer their pharmacokinetic properties. The Procheck online portal and Discovery Studio visualizer were used to validate the

receptors or protein structures that were taken into consideration in the docking investigations. For the in vitro antibacterial investigation, the disc diffusion assay was used against two strains of bacteria that are non-pathogenic in nature. The investigation revealed somewhat strong antibacterial activity, and MIC calculations were also performed. Total phenolic, flavonoid and terpenoid content were quantitatively estimated from the obtained extract. Antioxidant activity of the plant extract also had been performed by using the peroxide method. IMODS web portal was used for the simulation study of the selected receptor.

Key Words: *In-silico* study, PyRx, Phenolic content, discovery studio visualizer, *Acacia suma* L.

1. INTRODUCTION

The use of herbal heritage has become a part of general health care. The use of modern medicines of synthetic origin imparting dramatic results in a short span in the therapeutic field laid several side effects upon long term use. Traditional medicaments, chiefly obtained from plants have played a vital role in sustaining disease free human existence on this plant [1]. Plant-derived material can have an effective and positive role in the treatment of damaged cells during wounding healing. In Indian traditional systems of medicine, plants have been used by traditional practitioners [2]. To speed up drug research and to improve success rates, research costs should be decreased. Computer-aided drug design (CADD) has become an important means of designing new drugs [3].

According to ethnopharmacological research, *A. suma* stem bark preparations are used in a number of traditional and folkloric medical systems worldwide like in treating local sores, gonorrhoeae, pneumonia, leprosy, malaria, diabetes and regarded as aphrodisiac [4]. The plant possesses bitter, astringent, and thermogenic properties. It has been shown in several experimental setups to have analgesic, anthelmintic, anti-inflammatory and wound healing [5].

Among varieties of herbal plants that grow around us, *Acacia suma* L. is one of those plants having various ethnomedicinal and pharmacological uses and therefore its antimicrobial, anticoagulant as well as antioxidant activity are performed and explained. To accelerate drug research and to improve success rates, research costs should be decreased. Computer-aided drug design (CADD) has become an important means of designing new drugs [6].

The experimental work in this study has been concentrated on the antioxidation, antibacterial, and *in-silico* antibacterial examination of the chloroform extract of ***Acacia suma* L**. plant constituents due to the dearth of scientific evidence.

2. MATERIAL AND METHODS

Materials

The extraction procedure made use of methanol (Merck, India), ethanol (Lobachem, India), and chloroform (Lobachem, India). The phenolic content of the extract was estimated using gallic acid (Lobachem, India), the Folin-Ciocalteu Reagent (Lobachem, India), and hydrogen peroxide (Merck, India) was employed for the peroxide method of antioxidant research. Chloroform extracts were tested against a panel of two non-pathogenic bacterial strains including *Staphylococcus Aureus* MTCC NO. 87 and *Pseudomonas aerugenosa* MTCC NO. 424 that were purchased from Institute of Microbial Technology, Sector 39, Chandigarh, India.

Preparation of extract

The plant sample, which consisted of leaves, was gathered and it was then air dried in the shade at room temperature, grounded into a fine powder with an electric grinder, and then stored in an airtight container for future use. For extraction, the powdered sample was combined with solvents in a 4:1 methanol to water ratio. The substance was then filtered using Whatman No. 1 filter paper, and the filtrate was combined with (2–3) drops of 2M HCl before being combined with an equivalent volume of chloroform. The dried residue was obtained by taking the lower organic layer after it had formed, separated, and then the solvent was evaporated. The organic layer by mechanism is supposed to have flavonoids/phenolic/terpenoids fraction of the extract which then was mixed with distilled water and 1% w/v of Tween 80 solution for further antibacterial and antioxidant activity [7].

Preliminary phytochemical screening

The extracts was subjected to preliminary phytochemical screening for the detection of various phytoconstituents using standard procedures:

Test for Alkaloids

Approximately 5 mg of the extract was dissolved in 5 ml of distilled water and 2ml of HCl was added until complete precipitation and filtered. The filtrate was tested for the presence of alkaloids as below.

a) Dragandroff's test: 1ml of Dragandroff's reagent was added to 2ml of the filtrate along the side of the test tube. Formation of a reddish brown precipitate indicated the presence of alkaloid.

b) Wagner's test: Two drops of Wagner's reagent was added to 1ml of the test solution along the side of the test tube. The formation of yellow or brown precipitate confirmed the presence of alkaloids.

Test for Flavonoids: Small quantity of each extract was heated with 10ml of ethyl acetate in boiling water bath for 3 minutes. The mixture was filtered and filtrates are used for the following tests.

a) Ammonium test: the filtrate was shaken with dilute ammonia solution (1ml, 1%, v/v). The layers were allowed to separate. A yellow colour observed at ammonia layer indicated the presence of flavonoid.

b) Alkaline reagent test: The extract (2ml) was treated with few drops of 20% (w/v) NaOH solution. Formation of intense yellow colour, which turned colourless on the addition of dilute HCl indicated the presence of flavonoids.

c) Shinoda test: A few magnesium turnings and 5 drops of concentrated hydrochloric acid were added drop wise to 1ml of test solution. A crimson red colour appeared after few minutes confirmed the presence of flavonoid.

Test for Phytosterols/ Terpenoids

Liebermann-Burchard's test: 2 mg of the extract was dissolved in 2ml of acetic acid anhydride, heated to boiling, cooled and then 1ml of concentrated sulphuric acid was added along the side test tube. A brown ring formation at the junction confirmed the test for the presence of phytosterols.

Test for Tannin

Ferric chloride test: A few drops of 5% (w/v) $FeCl_3$ solution was added to the test solution (2ml). Formation of bluish black colour indicated the presence of hydrolysable tannin.

Test for Glycosides

Felling test: A few drops sulphuric acid was added to the test solution (2ml) and then 5% NaOH solution was added for neutralization process into it. Finally, Fehling's solutions A and B were added to the above mixture. The solution produces a red colour to indicate the positive result.

Test for Phenol

Extracts were treated with 3-4 drops of 10% (w/v) $FeCl_3$ solution. Formation of greenish black colour indicates the presence of phenol.

Test for Triterpenoid

Salkowski test: Dry extracts (2mg) was shaken with chloroform (1ml) and a few drops of Conc. H_2SO_4 were added along the side of the test tube. A red-brown colour formed at the interface indicated the presence of triterpenoid [8].

Estimation of the Total Phenolic Content

A series of gallic acid standard solutions of 10, 20, 30, 40, 50 µg/ml were prepared in test tubes and 1 mL of Folin-Ciocalteu reagent was added to each tube and mixed well. After exactly 5 minutes, 1 mL of 7% sodium carbonate solution was added to each tube or and mixed thoroughly. The solutions were allowed to stand for 2 hours at room temperature, protecting them from light. The absorbance of each solution was measured at 765 nm using UV spectroscopy. A standard curve was prepared by plotting the concentration of gallic acid (µg/mL) on the x-axis and the corresponding absorbance values on the y-axis. 100 mg sample was weighed and transferred into a test tube. A suitable solvent ethanol or water was added to the test tube to extract the phenolic compounds. The contents were thoroughly mixed and allowed the extraction to proceed for 30 minutes with occasional shaking. The sample extract was centrifuged at a suitable speed and duration to remove any insoluble particles. The supernatant extract was transferred to a new test tube, which was used for analysis. The absorbance of this solution was measured by UV spectroscopy. Calculate the total percentage phenolic content of the sample using the equation obtained from the standard curve. The value obtained of the total flavonoid content were expressed as milligrams of gallic acid equivalent per 100 mg of dry mass [9].

Estimation of the Total Flavonoid Content

Aluminium chloride colorimetric assay was used to measure the total flavonoid content of the extract. A 10 ml volumetric flask keeping 4 ml of distilled deionized water was filled with a portion (1 ml) of extracts or a standard solution of (+)-quercetin (20, 40, 60, 80, 100 µg/ml). 0.3 ml of 5% $NaNO_2$ was put in to the flask. 0.3 milliliter of 10% $AlCl_3$ was added after 5 minutes. Following addition of 2 milliliters of 1 M NaOH at the sixth minute, the volume was raised to 10 milliliters using deionized water. The solution was thoroughly mixed, and a Shimadzu UV-Visible spectrophotometer was used to measure the absorbance against a prepared reagent blank at 510 nm with a UV-Visible spectrophotometer. The value obtained of the total flavonoid content were expressed as milligrams of (±) quercetin equivalent (QE) per 100 mg of dry mass [10].

Determination of total terpenoids content (TTC)

200 µl of extract solutions in methanol (0.1 mg/ml) was first mixed with 1 ml of perchloric acid and 300 µl vanillin/glacial acetic acid (5% w/v) solution. 5 ml of glacial acetic acid was then added to it and the absorbance was measured at 548 nm

with a Shimadzu UV-Visible spectrophotometer. Ursolic acid at concentrations (20, 40, 60, 80, 100 µg/ml) were used to generate the standard calibration curve [11].

Evaluation of antimicrobial activity

Antimicrobial assessment Broth dilution method

The minimum inhibitory concentration (MIC) was determined using the broth dilution method as described by a specific method [12]. Specific concentration of extract dilutions were prepared using tubes containing 4 ml of double strength broth and with 0.5ml of inoculums. In all test tubes, test antimicrobial compound is added in the amount of 0.5ml except uninoculated (negative control) and control (positive) tube. The positive control tube is to check for the suitability of the test microorganism and the viability of the inoculums. The final volume was adjusted in all tubes by using sterile water. The tubes were inoculated with the suspension of standardized inocula (0.5 McFarland standard) and incubated at 37°C for 24 h. MIC was recorded as the lowest concentration of extract showing no visible bacterial growth.

Disc diffusion method

The disc diffusion assay will be used to screen for antibacterial activity as described by scientists [13]. The standard inoculum will be introduced onto the surface of the sterile agar plates and a sterile glass spreader was used for even distribution over the media. Blank sterile paper discs (6 mm) will be placed on the inoculated Mueller-Hinton agar surface and impregnated with 50 µl of the different extracts. A concentration of 10 µg/disc of Streptomycin (Sigma Aldrich, India), will be used as a standard. The procedure shall be repeated for all the selected bacterial species used. The plates shall be incubated at 37°C for 24 h. All tests will be performed in triplicate and the antibacterial activity will be expressed as the mean diameter of inhibition zones (mm) produced by the extracts.

Evaluation of Anti-oxidant activity

A test tube, a fixed volume of 2.5 ml of 1 mM hydrogen peroxide was added and to another test tube a fixed volume of sample dilution 0.5 ml containing the hydrogen peroxide solution. A control tube was included with only the hydrogen peroxide solution without the sample to measure the background reaction. All the reaction mixtures were incubated at a specific temperature for 30 minutes to allow the reaction to proceed. After the incubation period, a suitable stop solution was added to terminate the reaction. Commonly used stop solutions include sulphuric acid, sodium hydroxide, or catalase enzyme. The absorbance of each reaction mixture was measured using a spectrophotometer at 230 nm that corresponds to the absorption peak of hydrogen peroxide. Subtracted the absorbance of the control from the absorbance of each sample to obtain the net absorbance. Ascorbic acid was used as standard compound.

Antioxidant activity (%) = $[(A_0 – A_1) / A_0] \times 100$; Where A_0 is the absorbance of the plant extract and A_1 is the absorbance of the plant-peroxide sample [14].

In Silico study for assessment of antibacterial activity

In-silico study

Molecular docking method has been employed here to find out the binding affinity (docking score) between the reported active phytoconstituents (Flavonoids/Phenolic/terpenoids) of the plant extract that served the purpose as a ligand and the microbial protein that was designated as the receptor site or active binding site to have the successfully inhibition of the microbes for the purpose of possible antimicrobial activity.

Protein preparation

In the present study, as per the reported mechanism of action of the selected phytoconstituents (ligand), Receptors were selected as bacterial ***(S. aureus, Pseudomonas aeruginosa)*** target protein as it plays important role in the life cycle of bacteria and it was obtained from the RCSB PDB database for the docking study. The protein was then processed by eliminating water molecules, internal ligands, removing superfluous chains or heteroatoms, introducing polar hydrogen charges in Discovery Studio Visualizer. After that it was open in PyRx (Algorithm is same as Auto Dock Vina) and was converted to PDBqt format. Ultimately, the ligand was then placed in the centre of the grid box and the docking process was performed in the presence of previously prepared ligand molecule.

Receptors or protein structures that were taken part in the docking studies were validated with discovery studio visualizer and **procheck** web portal.

Ligand preparation

The bioactive ligand molecules, **Quercetin and Kaempferol** were selected on the basis of it's docking score with the specific receptors and downloaded from the PubChem directory as 3D Standard Data Format (3D SDF) format. OPEN BABEL interface was used to translate the ligand from 3D SDF files to Protein Data Bank (PDB) format. These ligand molecules were independently uploaded into the AutoDock Tools (PyRx) during ligand preparation. It was prepared by minimizing the energy of the structure and also by converting it to PDBqt format for the evaluation of the binding affinity (docking score) of the receptor-ligand complex.

Visualization of the Structure

After the completion of the docking process in the PyRx software best fit of the ligand structure to the receptor surface was identified having the docking score of less than -7 and RMSD value of 0. It was then placed in the prepared protein structure placed on Discovery Studio Visualizer and interaction parameters (Hydrogen Bond formation with residues, distance, Donor-acceptor properties etc.) were examined and all the non-bond parameters were recorded. The 3-dimensional and 2-dimensional structures of the complex was noted.

In-silico study will be carried out with the reported flavonoid/polyphenolic part (ligand) of the plant extracts against the microorganism (Protein/receptor or specific enzyme) used in the in-vitro study with the help of BIOVIA DISCOVERY STUDIO and AUTODOCK VINA (PyRx) software for the evaluation of specific parameters which will be needed for the completion of the study.

Plant name	**Reported isolated compound (Ligand)**	**Activity**	**Microorganism**	**Protein/Receptor name**	**Protein/Receptor specification**
Acacia suma	Gallic acid	Antibacterial	*S. aureus*	Integrase [15]	3NKH
	Catechin	Antibacterial	*S. aureus*	DNA gyrase [16]	5CDN
			Pseudomonas aeruginosa	DNA gyrase [16]	7PTG
	Quercetin	Antibacterial	*S. aureus*	ILE TRNA synthetase [17]	1FFY
				Glycosyltransferase[18]	3VMR
			Pseudomonas aeruginosa	3-oxyacyl-[acyl carrier protein] reductase [19]	4BO3
				enoyl-acyl carrier protein reductase [20]	4NR0
	β-sitosterol	Antibacterial	*S. aureus*	Sortase B [21]	1QWZ
			Pseudomonas aeruginosa	Virulence factor regulator [22]	2OZ6
	Kaempferol	Antibacterial	*S. aureus*	Active helicase [23]	5DGK
				DNA helicase sapria [24]	5XGT
		Antibacterial	*Pseudomonas aeruginosa*	3-oxyacyl-[acyl carrier protein] reductase [19]	4BO3
				enoyl-acyl carrier protein reductase [25]	4NR0

Table 1: *In-silico* study

D.S- Docking Score (PyRx), RMSD- Interaction Energy (PyRx), DIAGRAM (DISCOVERY STUDIO)

The Ramachandran plot

An easy technique to view the distribution of torsion angles of protein structure is to use the two torsion angles of polypeptide chain, which characterise the rotation of the polypeptide backbone around the bonds between N-Cα called phi (φ) and Cα-C called shi (ψ).

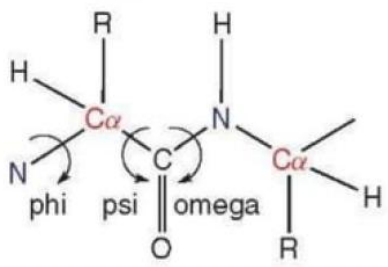

Fig 1: phi and psi angle in structure of proteins

One of the most crucial local structural factors that regulates protein folding and is a good measure of the integrity of a protein's three-dimensional structure is its torsion angle. The Ramachandran Plot is a useful tool for understanding the structural accuracy of protein conformations. It plots the phi (υ) and psi (ψ) dihedral angles of amino acid residues, which helps to assess the stereochemical quality of protein structures. Because the partial-double bond keeps the peptide bond planar, the ω angle at that specific peptide bond is always 180 degrees.

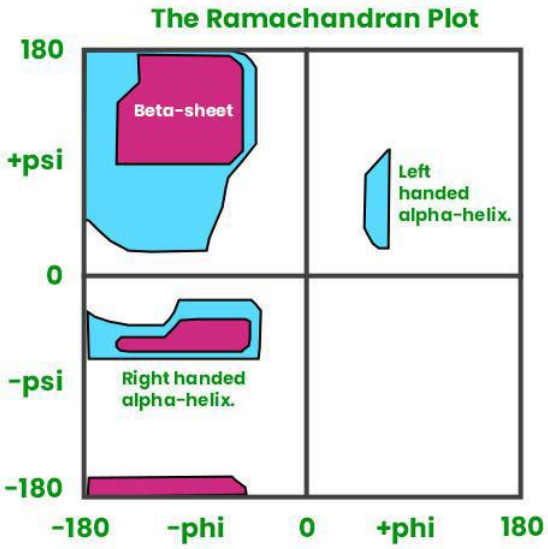

Fig 2: Ramachandran plot

Ramachandran Plot Quadrants

The Ramachandran plot, which has four quadrants, can be used to determine the secondary structure of proteins.

Quadrant-I: The left-handed alpha is found in the confirmations area (Quadrant-I), where all confirmations are permitted.

Quadrant II: This is the largest section on the graph overall, and it offers the best conditions for atom confirmation.

Quadrant-III: This sector, which is the largest after Quadrant-II, contains right-handed alpha.

Quadrant-IV: This conformation (ψ around 0-180 degrees, ψ around 180 degrees) is not preferred because of steric conflict. It has almost no framed locale.

Secondary Structure Plot

The two most common examples of secondary structures in the Ramachandran plot are α-helix and β-sheets, which are discussed in detail below. Secondary structures are small, repeating building blocks of peptides that look the same because the amino acid building blocks have similar angles. By checking these angles on the Ramachandran plot, we can tell different secondary structures apart.

α-helix

The polypeptide chain coils tightly around a central axis and is stabilised by hydrogen bonds between particular amino acid residues to form an alpha helix, a right-handed helical coiled structure that is essential for the proper folding and function of proteins. The regular backbone conformation of the alpha helix is represented in a Ramachandran plot by a

distinct region that is defined by specific angles (phi and psi) that correspond to the hydrogen bonding pattern that repeats in the alpha helix structure. This region usually falls within a narrow range of phi and psi angles.

β-sheets

In proteins, beta sheets are secondary structures made up of contiguous polypeptide chain strands that are oriented side by side and kept stable by hydrogen bonds between their backbone atoms. Specific sections that match the distinctive phi and psi angles connected to the regular arrangement of amino acid residues in beta strands are used to represent beta sheets in a Ramachandran plot.

Preferences of Amino Acids

Larger side chains would impose further restrictions and lead to a smaller permissible region in the Ramachandran plot, but their effect is negligible; the methylene group's presence or absence at Cβ is found to have the most impact.

Since glycine's side chain contains only one hydrogen atom, it has a smaller van der Waals radius than other amino acids, which results in a less constrained conformational space, as shown by its Ramachandran plot. Proline, on the other hand, has a 5-membered ring side chain that connects Cα to backbone N, which means that there are fewer possible combinations of ψ and ψ in its Ramachandran plot than in the general case. The residues that come before Proline, or "Pre-Proline," also display fewer possible combinations than in the general case.

In conclusion, the Ramachandran Plot is a valuable tool for understanding protein structure through the analysis of allowed and disallowed regions of phi (υ) and psi (ψ) angles. It plays a critical role in protein modelling and drug design by helping scientists confirm protein structures, improve accuracy, and identify errors. However, despite its many applications, the Ramachandran Plot has some limitations that emphasise the importance of careful interpretation in structural biology research.

ADME analysis **[26]**

The ADME analysis (physicochemical properties, water solubility, lipophilicity, pharmacokinetics, drug likeness and medicinal chemistry) of the phytoconstituents tested (Catechin) was carried out by Swiss ADME software.

3. RESULT & DISCUSSION

Phytochemical Screening

Experimental Plant- ***Acacia suma*** **L.**

Terpenoids	***Alkaloids Test***		***Glycoside***	***Flavonoids***		***Steroid***	***Phenol***	***Tannin***
Salkowski test	Dragendorff	Wagner	Fehling test	Shinoda test	Alkaline reagent	Salkowski test	10% Ferric Chloride test	5% Ferric Chloride test
-	+	+	+	+	+	-	+	+

Table 2: Phytochemical screening of *Acacia suma* leaves extract

Positive Control- Tulsi (*Ocimum sanctum)*

Terpenoids	***Alkaloids Test***		***Glycoside***	***Flavonoids***		***Steroid***	***Phenol***	***Tannin***
Salkowski test	Dragendorff	Wagner	Fehling test	Shinoda test	Alkaline reagent	Salkowski test	10% Ferric Chloride test	5% Ferric Chloride test
+	+	+	+	+	+	+	+	+

Table 3: Phytochemical screening of *Ocimum sanctum* leave extract

Ocimum sanctum was chosen as the positive control plant for the validation of the chemicals was used in phytochemical screening.

The above result indicates that the final extract residue contains primarily the flavonoids/phenolic group, which was one of the experimental objectives which was further screened through by LC-MS/MS study of the plant extract.

Name	R. Time (min)	Formula	Mass Error (ppm)	Calc. Molecular Mass	Database	Matching Score (MzCloud)/ FISh Score (Chemspider)	Class
Luteolin 7-O-malonylglucoside	6.22	$C_{24}H_{22}O_{14}$	0.31	534.1011	ChemSpider	62.5	Flavonoid
Nicotiflorin	5.85	$C_{27}H_{30}O_{15}$	0.45	594.1587	mzCloud	99.4	Flavonoid
Quercetin	5.07	$C_{15}H_{10}O_7$	−1.22	302.0423	mzCloud	99.4	Flavonoid
Quercetin 3-O-rhamnoside-7-O-glucoside	5.54	$C_{27}H_{30}O_{16}$	−0.33	610.1532	mzCloud	98.2	Flavonoid
Quercetin-3β-D-glucoside	5.67	$C_{21}H_{20}O_{12}$	−0.33	464.0953	mzCloud	96.8	Flavonoid
Robinin	5.48	$C_{33}H_{40}O_{19}$	0.40	740.2167	mzCloud	97.2	Flavonoid
Trifolin	5.99	$C_{21}H_{20}O_{11}$	−0.55	448.1003	mzCloud	98.2	Flavonoid
Adenine	2.15	$C_5H_5N_5$	0.08	135.0545	mzCloud	89.3	Heterocyclic
Adenosine	2.15	$C_{10}H_{13}N_5O_4$	−0.21	267.0967	mzCloud	99.8	Heterocyclic
Coniine	21.44	$C_8H_{17}N$	−0.04	127.1361	ChemSpider	52.9	Heterocyclic
Guanine	21.56	$C_5H_5N_5O$	−0.30	151.0494	mzCloud	95.4	Heterocyclic
(3S,4R,5R,6R)-6-[(4R)-2,2-Dimethyl-1,3-dioxolan-4-yl]-3,4-dihydroxy-5-methyltetrahydro-2H-pyran-2-one	2.94	$C_{11}H_{18}O_6$	−1.05	246.1101	ChemSpider	52.4	Lactone
Massoilactone	5.89	$C_{10}H_{16}O_2$	−0.41	168.1150	ChemSpider	65.0	Lactone
Albocyclin	6.53	$C_{18}H_{28}O_4$	−0.53	308.1986	ChemSpider	61.1	Macrolide
Rustmicin	6.48	$C_{21}H_{32}O_6$	−1.59	380.2193	ChemSpider	52.2	Macrolide
1-(4-Hydroxy-3-methoxyphenyl)-5-methoxy-3-decanone	6.77	$C_{18}H_{28}O_4$	−1.03	308.1984	ChemSpider	69.1	Phenolic

(12S)-12-Hydroxy-16-heptadecynoic acid	10.81	$C_{17}H_{30}O_3$	−0.10	282.2195	ChemSpider	53.9	Fatty acyl
(2E)-6-Hydroxy-2,6-dimethyl-2,7-octadienoic acid	5.09	$C_{10}H_{16}O_3$	0.48	184.1100	ChemSpider	54.6	Fatty acyl
1-[(2-Hydroxyethyl)amino]-2-dodecanol	21.44	$C_{14}H_{31}NO_2$	−0.33	245.2354	ChemSpider	55.6	Fatty acyl
11-Methoxy-3,7,11-trimethyl-2,4-dodecadienoic acid	8.43	$C_{16}H_{28}O_3$	−0.12	268.2038	ChemSpider	65.9	Fatty acyl
13-Hydroxy-9,11,15-octadecatrienoic acid	8.52	$C_{18}H_{30}O_3$	−0.40	294.2194	mzCloud	85.4	Fatty acyl
4-Oxo-dodecanedioic acid	6.44	$C_{12}H_{20}O_5$	−0.52	244.1310	mzCloud	80.2	Fatty acyl
Arachidonic acid	7.01	$C_{20}H_{32}O_2$	−0.98	304.2399	ChemSpider	90.5	Fatty acyl
Levulinic acid	1.10	$C_5H_8O_3$	1.96	116.0476	ChemSpider	62.5	Fatty acyl
Palmitoleyl oleate	20.98	$C_{34}H_{64}O_2$	−0.03	504.4906	ChemSpider	85.8	Fatty acyl
Parinaric acid	11.45	$C_{18}H_{28}O_2$	−0.74	276.2087	ChemSpider	85.6	Fatty acyl
Traumatin	5.76	$C_{12}H_{20}O_3$	−0.11	212.1412	ChemSpider	56.4	Fatty acyl
2-(3,4-Dihydroxyphenyl)-5,7-dihydroxy-4-oxo-4H-chromen-3-yl 6-O-(carboxyacetyl)-β-D-threo-hexopyranoside	5.84	$C_{24}H_{22}O_{15}$	0.78	550.0963	mzCloud	99.0	Flavonoid
Kaempferol	5.35	$C_{15}H_{10}O_6$	−1.04	286.0474	mzCloud	98.2	Flavonoid

Table 4: Compounds identified in chloroform extract of plant leaves by positive mode of analysis

Quantitative Estimation of Phenolic Content

CONCENTRATION OF GALLIC ACID (µg/ml)	OBSERVED ABSORBANCE
10	0.0549
20	0.2396
30	0.6733
40	0.8652
50	0.9872

Table 5: Absorbance values of Gallic acid solution

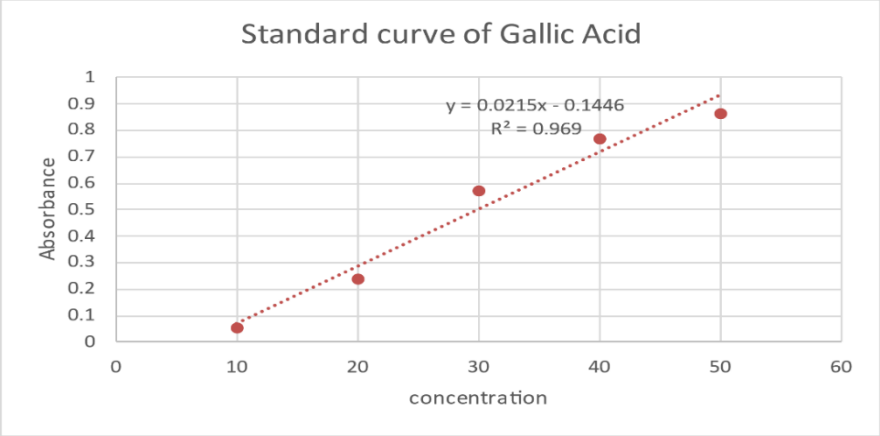

Fig 3: Standard curve of Gallic acid

From the standard curve this equation was found as y= 0.0215x-0.1446

The absorbance of extract of *Acacia suma* L. was: 0.7882

So, according to the equation the concentration of phenolic content of the extract was **43.39 µg/ml** equivalent to 100 mg of gallic acid.

Estimation of total Flavonoid content

CONCENTRATION OF QUERCETIN (µg/ml)	OBSERVED ABSORBANCE
20	0.0937
40	0.0966
60	0.1354
80	0.1651
100	0.2510

Table 6: Absorbance values of Quercetin Solution

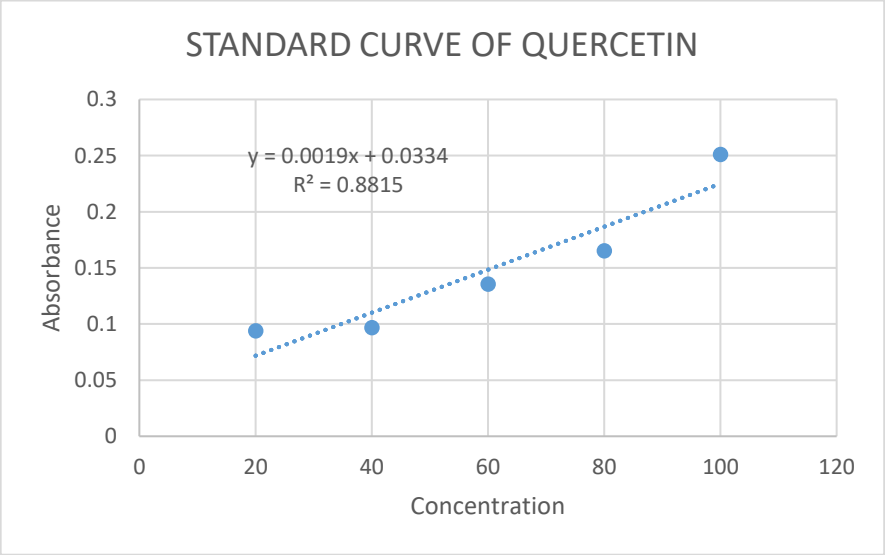

Fig 4: Standard curve of Quercetin

From the standard curve this equation was found as y= 0.0019x + 0.0334

The absorbance of extract of *Acacia suma* was: 0.1771

So, according to the equation the concentration of flavonoid content of the extract was **75.63 µg/ml** equivalent to 100 mg of quercetin.

Quantitative estimation of total terpenoid content (TTC)

CONCENTRATION OF URSOLIC ACID (µg/ml)	OBSERVED ABSORBANCE
10	0.0984
20	0.2124
30	0.4561
40	0.6658

50	0.8985

Table 7: Absorbance values of Ursolic Acid solution

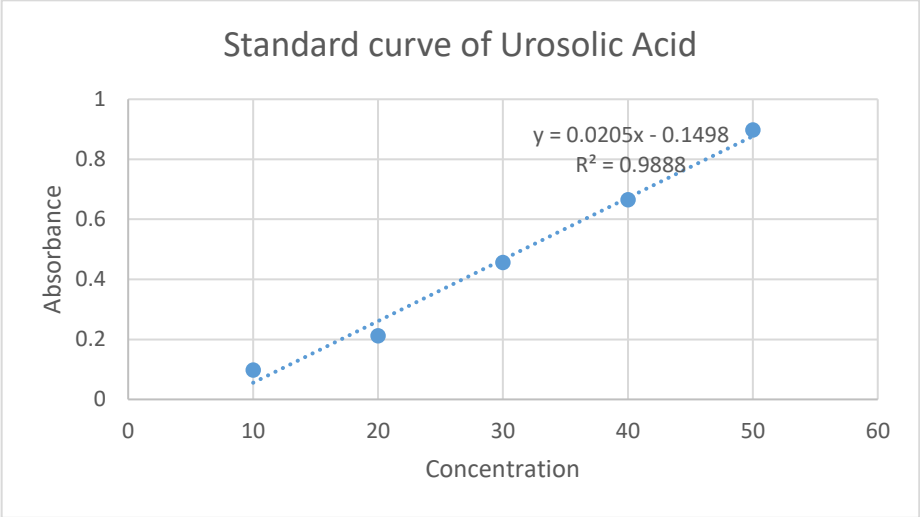

Fig 5: Standard Curve of Ursolic Acid

From the standard curve this equation was found as y= 0.0205x-0.1498

The absorbance value of the extract of *Acacia suma* was: 0.7958.

So, according to the equation the concentration of total terpenoid content of the extract was 46.12 µg/ml equivalent to 100 mg of Ursolic acid.

Evaluation of Antioxidant activity

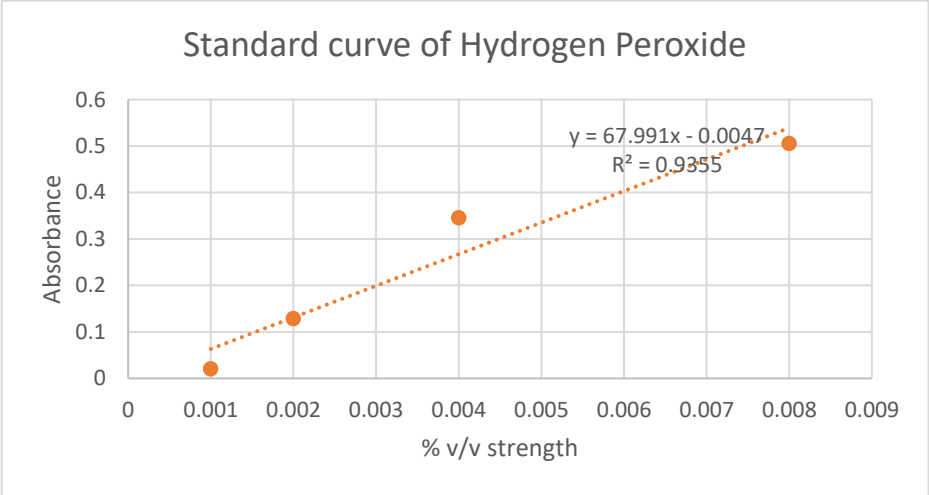

Fig 6: Standard curve of Hydrogen Peroxide

From the standard curve this equation has found y= 67.991x- 0.0047

The absorbance of extract of *Acacia suma* L. is: 0.45

Now % Scavenged due to extract solution is = $[(A_0 - A_1)/A_0]$ X 100

A_0= the absorbance of H_2O_2 sample = 0.96

A_1 = absorbance of mixture of plant sample and peroxide = 0.45

Percent Scavenged; % H_2O_2 = [(0.96−0.45) / 0.96] X 100

=53.12% (Moderate)

Similarly for the Ascorbic acid (Standard drug) it was found to be 52.9%.

Antibacterial Assessment

Microorganisms	Diameter of inhibition zone (mm)		MIC (mg/ml)
	Chloroform extract	Streptomycin	Chloroform extract
S. aureus	9.1 ± 0.33	9 ± 0.15	5
P. aerugenosa	10.10 ± 0.38	9.8 ± 0.25	4

Table 8: Assessment of Antibacterial activity of the plant extract

Note: The control disc used for solvent had no zone of inhibition, so there data was omitted from the above data. Inhibition zones including the diameter of the paper disc (6 mm). Results are expressed as the mean ± SEM of triplicate measurements.

The MIC of chloroform extract of ***Acacia suma*** were 5 mg/ml and 4 mg/ml against S. aureus and P. aerogenosa. The MIC determination was performed in triplicate for each organism.

The chloroform extract exhibited (Table 8) potent anti-bacterial activity against S. aureus (9.1 ± 0.33 mm) and P. aerugenosa (10.10 ± 0.38 mm). The same for the standard drug was found to be (9 ± 0.15 mm) and (9.8 ± 0.25 mm) against S. aureus and P. aerugenosa respectively.

The chloroform extracts of ***Acacia suma* L.** was produced antibacterial activity against all the tested organisms i.e. gram-negative bacteria (P. aerugenosa) and gram-positive bacteria (S. aureus).

***IN-SILICO* STUDY**

PDB ID: 1FFY

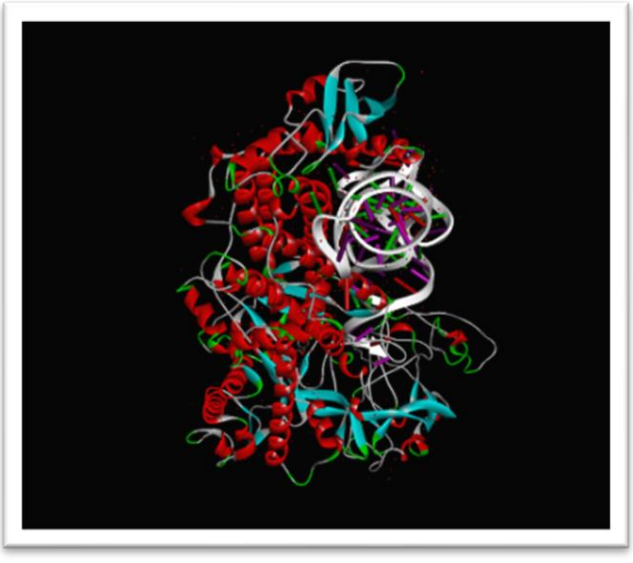

Fig 7: Protein structure of binding site data base code (1FFY)

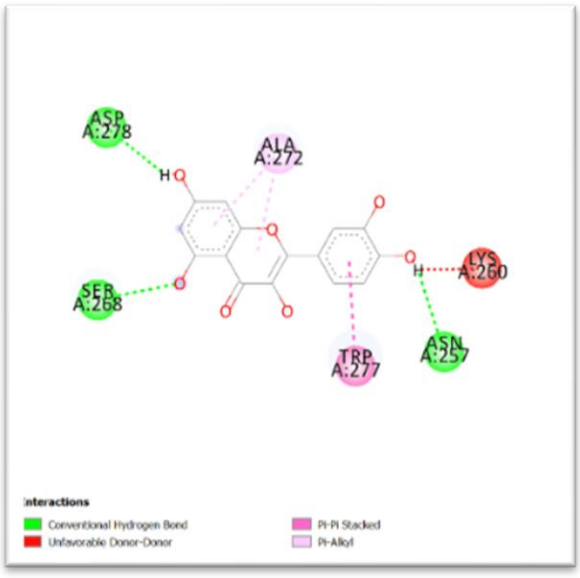

Hydrogen-bond interacting active binding site residues: **ASN 257, ASP 258, SER 268**

Fig 8: 2D diagram of Quercetin- 1FFY complex best fit interaction

PDB ID: 4NR0

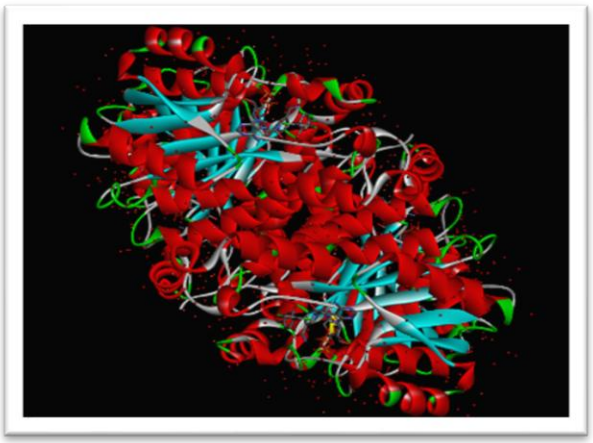

Fig 9: Protein structure of binding site data base code (4NR0)

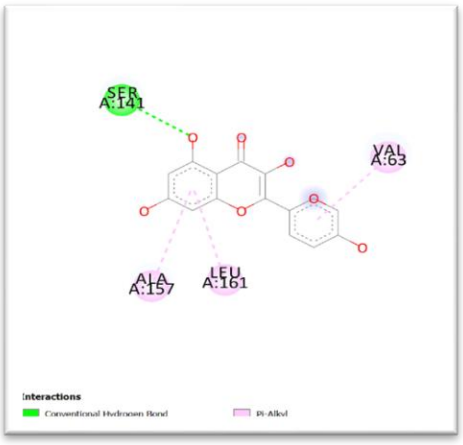

Hydrogen-bond interacting active binding site residues: **SER 141**

Fig 10: 2D diagram of Quercetin- 4NR0 complex best fit interaction

PDB ID: 5DGK

Fig 11: Protein structure of binding site data base code (5DGK)

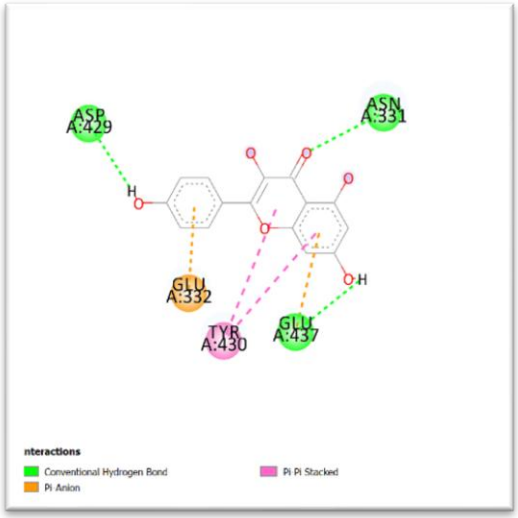

Hydrogen-bond interacting active binding site residues: **ASP 429, GLU 437, ASN 331**

Fig 12: 2D diagram of Kaempferol- 5DGK complex best fit interaction

PDB ID: $4BO_3$

Fig 13: Protein structure of binding site data base code ($4BO_3$)

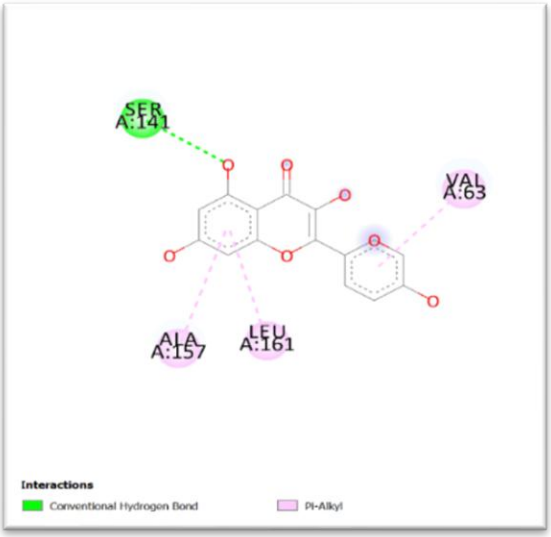

Hydrogen-bond interacting active binding site residues: **SER 141**

Fig 14: 2D diagram of Kaempferol - $4BO_3$ complex best fit interaction

LIGAND	RECEPTOR	MICROORGANISM	DOCKING SCORE (Best fit)	RMSD VALUE
Reported Test Compound (**Quercetin**)	1FFY	*S. aureus*	**-9.5**	0
Standard Compound (Gentamycin)			**-6.9**	0
Reported Test Compound (**Quercetin**)	4NRO	*P. aeruginosa*	**-8.9**	0
Standard Compound (Gentamycin)			**-7.8**	0
Reported Test Compound **(Kaempferol)**	5DGK	*S. aureus*	**-7.6**	0
Standard Compound (Gentamycin)			**-6.8**	0
Reported Test Compound **(Kaempferol)**	**$4BO_3$**	*P. aeruginosa*	**-7.7**	0
Standard Compound (Gentamycin)			**-6.5**	0

Table 9: Summary of Docking Study

ADME analysis

According to the above data, the plant extract claimed phytoconstituents like **Quercetin** and Kaempferol demonstrated more *in silico* antibacterial efficacy against *Pseudomonas aeruginosa* and *Staphylococcus aureus* than the standard drug Gentamycin and out of the both ligands Quercetin complex with receptor shows best docking score of the studies.

Quercetin

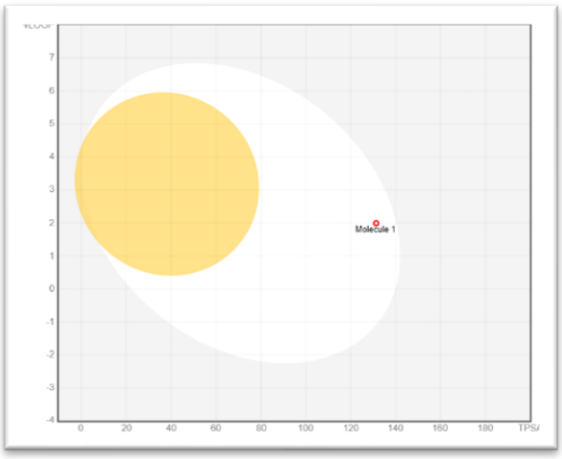

Fig 15: Boiled Egg model of Quercetin

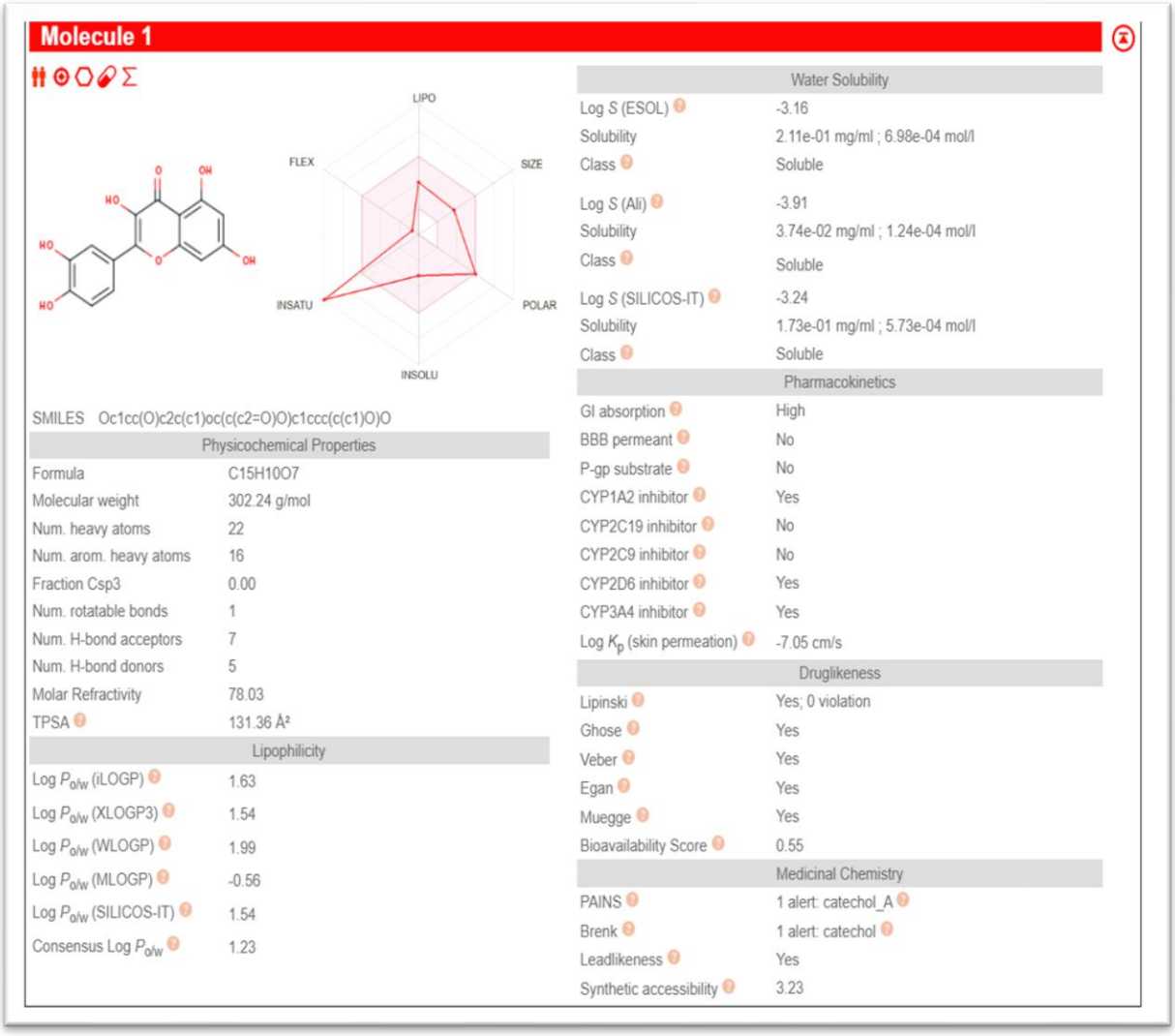

Fig 16: Structural details and physicochemical parameters of Quercetin

From the above figure it can be seen that Quercetin can cross the GI membrane & it also having good bio-availability score of 0.55 and it seemed to be obey Lipinski rules also.

Protein structure validation

1FFY

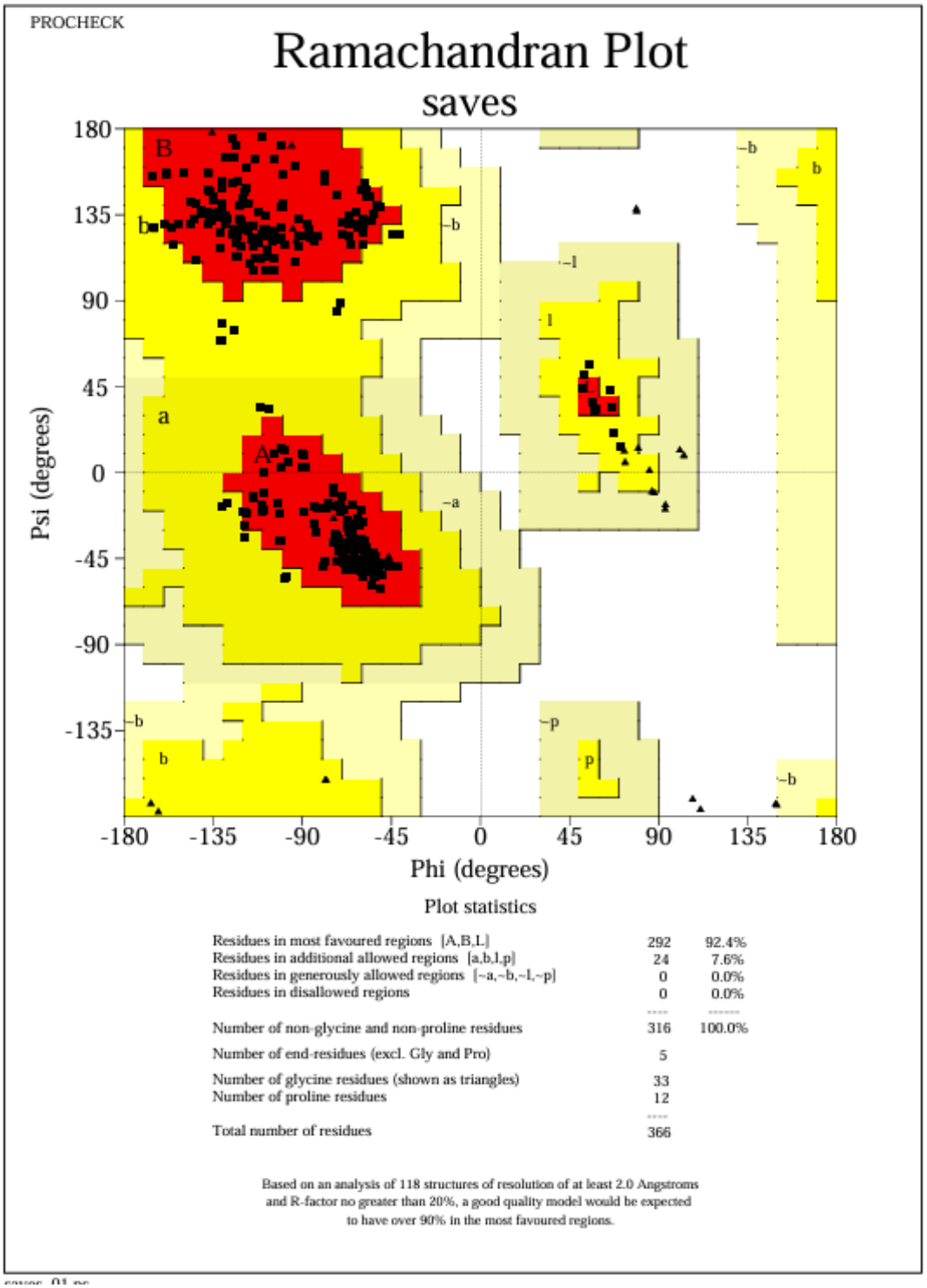

Fig 17: Ramachandran plot of 1FFY

Since the most liked area of the plot included more than 90% (92.4%) of the amino acid residue, receptor structure of 1FFY was validated and the model was approved as it was selected based on the best docking score observed when docked with quercetin.

Simulation Study **[27]**

Receptor PDB ID: 1FFY

β-factor/ Mobility

The main-chain deformability is a measure of the capability of a given molecule to deform at each of its residues during thermal oscillation with it's stability profile.

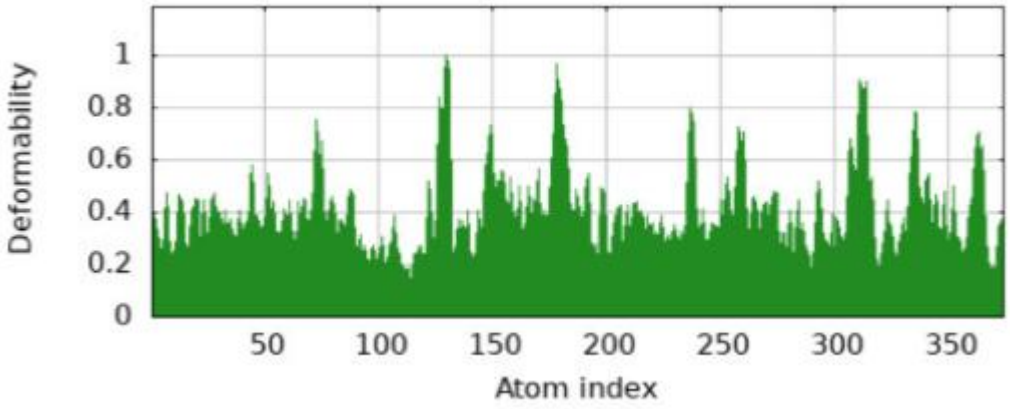

Fig 18: B-factor/ Mobility

Above figure indicates the number of amino acid residue present in the selected chain of the receptor.

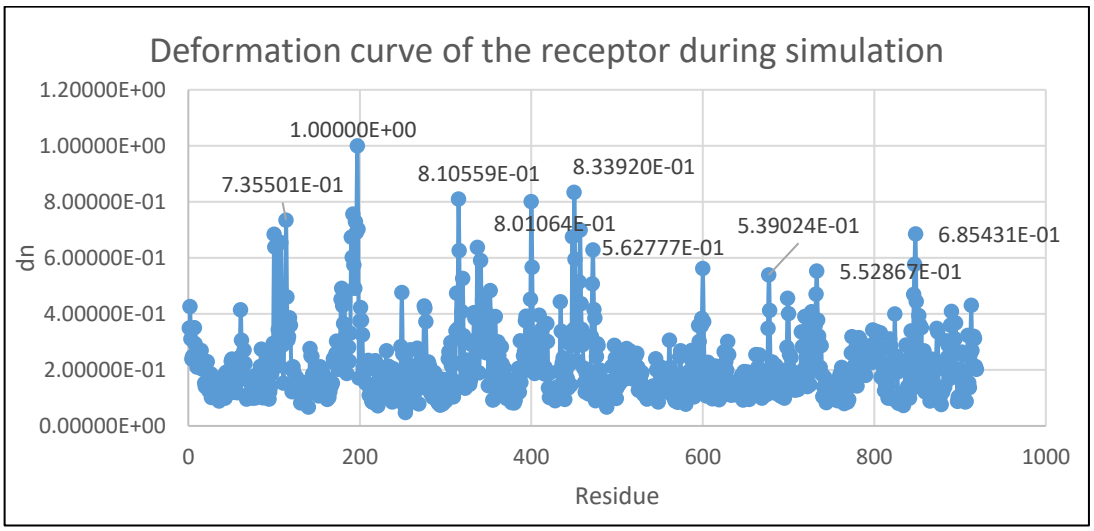

Fig 19: Deformability of amino acid residues

Also the highest/maximum deformability values of the amino acid in the above figure signifies the amino acids which will react with the ligand molecule.

r	dn	AMINO ACID	AMINO ACID FULL NAME
197	1.00000E+00	GLU197	Glutamic Acid
450	8.33920E-01	GLU450	Glutamic Acid
400	8.01064E-01	THR400	Threonine

315	8.10559E-01	VAL315	Valine
192	7.57152E-01	SER192	Serine
114	7.35501E-01	LYS114	Lysine
457	6.99310E-01	ARG457	Arginine
848	6.85431E-01	ALA848	Alanine
100	6.85101E-01	PRO100	Proline
337	6.37349E-01	VAL337	Valine
472	6.29123E-01	GLU472	Glutamic Acid
600	5.62777E-01	LEU600	Leucine
733	5.52867E-01	ARG733	Arginine
677	5.39024E-01	VAL677	Valine

Table 10: Deformability of amino acid residue

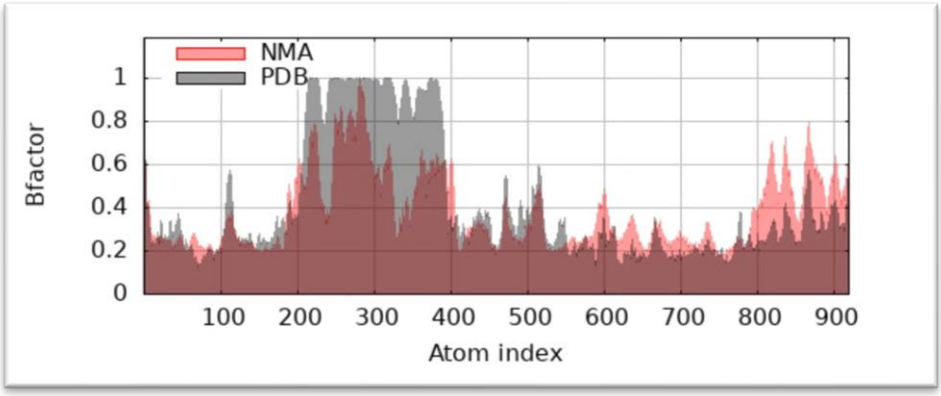

Fig 20: B-factor/ Mobility

Above figure shows the difference between PDB and NMA analysis. In general, experimental B-factors and NMA predicted mobilities are very similar.

NMA: Normal mode analysis

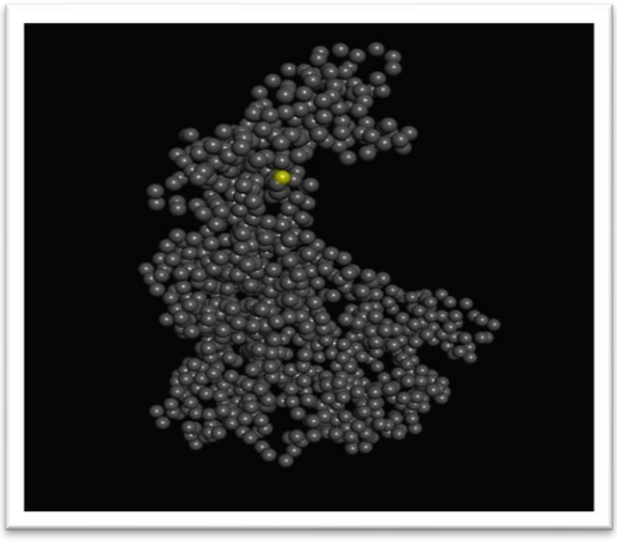

Fig 21: Deformability c-alpha chain of IFFY

Eigenvalues

The eigenvalue associated to each normal mode represents the motion stiffness. Its value is directly related to the energy required to deform the structure. The lower the eigenvalue, the easier the deformation.

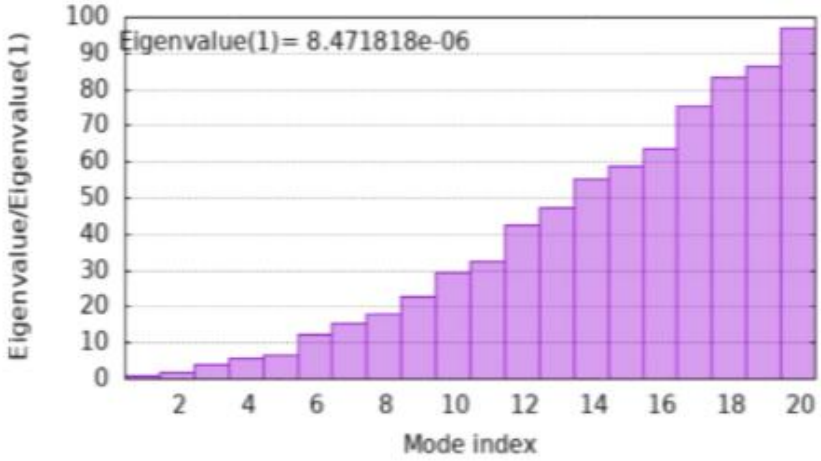

Fig 22: Eigenvalues of 1FFY

This figure represents the required energy, which is required for the deformation of the residue. Lower the value represents as the lower the energy, mean's that's easier for the deformation. This Eigen values plot evidences the relative modal stiffness.

MODE	EIGENVALUE
1	8.47182e-06
2	1.62382e-05
3	3.19891e-05
4	4.69816e-05
5	5.51601e-05
6	1.05625e-04
7	1.31052e-04
8	1.51809e-04
9	1.91707e-04
10	2.506526-04

Table 11: First ten Eigenvalues of 1FFY

	MODE	MAX_MOB	EIGENVALUE	MAX_DEF
MODE	1	3.466E+00	8.472E-06	4.721E-06
MODE	2	2.241E+00	1.624E-05	9.845E-06
MODE	3	1.562E+00	3.199E-05	8.148E-06
MODE	4	1.608E+00	4.698E-05	6.296E-06
MODE	5	1.138E+00	5.516E-05	7.471E-06
MODE	6	9.317E-01	1.056E-04	1.091E-05
MODE	7	7.106E-01	1.311E-04	9.104E-06

MODE	8	7.144E-01	1.518E-04	1.422E-05
MODE	9	7.345E-01	1.917E-04	1.264E-05
MODE	10	6.391E-01	2.507E-04	1.288E-05
MODE	11	5.342E-01	2.740E-04	1.593E-05
MODE	12	7.331E-01	3.598E-04	2.363E-05
MODE	13	5.484E-01	4.008E-04	1.777E-05
MODE	14	4.719E-01	4.664E-04	2.097E-05
MODE	15	6.047E-01	4.991E-04	1.811E-05
MODE	16	3.669E-01	5.383E-04	2.134E-05
MODE	17	6.410E-01	6.385E-04	2.346E-05
MODE	18	3.992E-01	7.050E-04	3.588E-05
MODE	19	4.788E-01	7.330E-04	3.363E-05
MODE	20	4.010E-01	8.212E-04	2.375E-05

Table 12: Computing deformability value of 1FFY

Variance

The variance associated to each normal mode is inversely related to the eigenvalue. Coloured bars show the individual (red) and cumulative (green) variances.

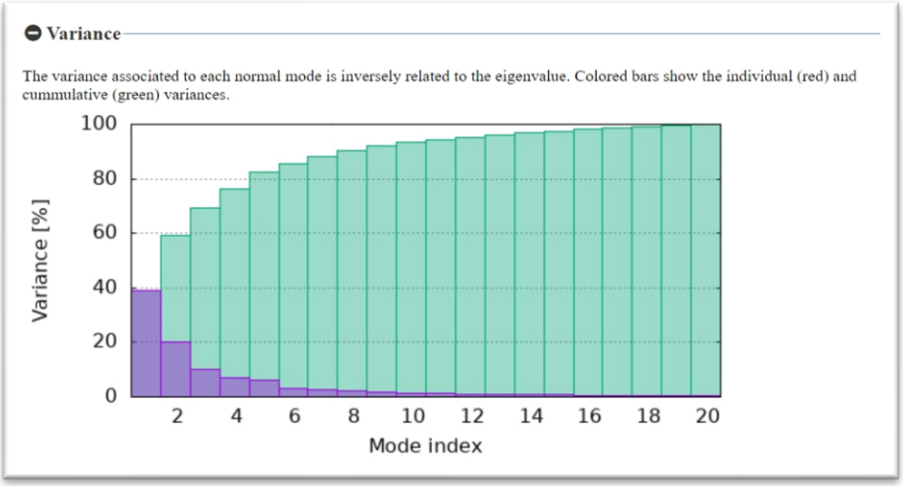

Fig 23: Variance of 1FFY

Above figure represents the reverse behaviour than Eigen values. The variance associated to the modes indicates their relative contribution to the equilibrium motions.

Covariance map

Covariance matrix indicates coupling between pairs of residues, i.e., whether they experience correlated (red), uncorrelated (white) or anti-correlated (blue) motions.

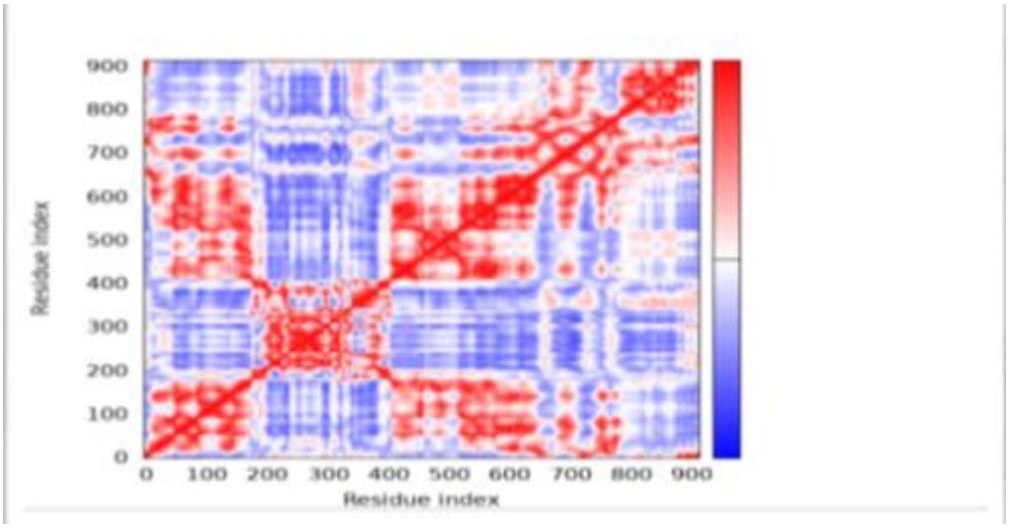

Fig 24: Covariance Map

Covariance matrix indicates which parts of the macromolecule move in a correlated, uncorrelated or anti-correlated fashion. Red colour shows the correlation between residue pairs, white shows no correlation and blue colour shows autocorrelations.

Elastic network

The elastic network model defines which pairs of atoms are connected by springs. Each dot in the graph represents one spring between the corresponding pairs of atoms. Dots are coloured according to their stiffness; the darker grey indicates stiffer spring and vice versa.

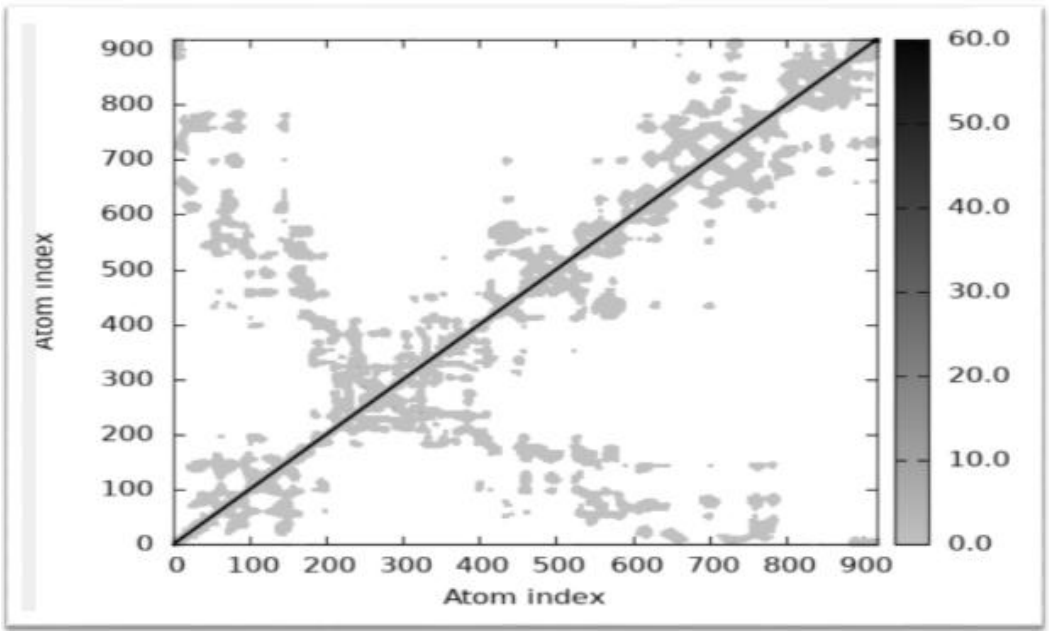

Fig 25: Elastic Network

The elastic network model used to compute the normal modes can be illustrated as a linking matrix.

SUMMARY:

Number of Molecules.....1
Number of Chain..... 1
Number of Segments..... 1
Number of Groups.....917
Number of Atoms 7407
Number of Hetero Mol. 0
Number of Hetero Atoms….....0

4. CONCLUSION

Currently, a number of conventional and folkloric medical systems employ medications that originate from the leaves of ***Acacia suma*** for treatment of different ailments in a random manner. These results could be used to distinguish this species from its other species diversity, identify the species using its pharmacognostic features, and assist in the creation of an herbal monograph for the species. Moreover, the findings of this study indicated that the phytochemical screening and LC-MS/MS study of the chloroform extract of leaves of ***Acacia suma*** confirmed the presence of Phenolic/Flavonoid/terpenoids fraction mainly due to which quercetin and kaempferol were selected for the *in-silico* study based on the reported phytoconstituents present on the plant leaves. In addition, same extract has a considerable amount of antibacterial activity against different non- pathogenic species when compared with the standard drug. Additionally, the plant extract exhibited spectrophotometrically determined antioxidant activity, which may result in the scavenging of free radical forms inside the biological systems. Also, the quantitative estimation of total phenolic content gave satisfactory result that may affect the antioxidant and antibacterial properties. An *in-silico* investigation has been conducted for all ligands against specific receptor types present in two different bacterial species which showed good binding affinity by forming hydrogen bonds with the interacting residues. The validated result of the receptor protein entity used for the *in-silico* study showed the presence of majority of amino acid presence in the allowed region that may be responsible for good docking score. The protein structure was validated with the help of Procheck using Ramachandran plot and SWISS ADME portal confirmed the drug likeness property of the reported ligand molecules along with the other satisfactory results during the *in-silico* study. Furthermore, simulation study was carried out using its respective portal to find out the B- factor or mobility as well as amino acid deformability, Eigen values, covariance and its elastic network of the receptor.

Future research can use the GC-MS method to separate and identify other fractions of plant extract, with the quantification of the extract by HPLC technique. The *in-vitro* MIC values of separated phytoconstituents can be compared with the *in-silico* docking score against the same set of bacterial strains that may be compared against the same standard ligand molecule.

ACKNOWLEDGEMET

The authors are sincerely thankful to the respected principal sir Dr. Arnab Samanta for providing the necessary facility for the completion of the research work.

REFERENCE

1. S. K. Mengane, "Antifungal activity of the crude extracts of Colocasia esculenta leaves in vitro on plant pathogenic fungi," International Research Journal of Pharmacy, 2015, Vol. 6, Issue 10, pp. 713-714.
2. Nakade Dhanraj B, Mahesh S. Kadam, Kiran N. Patil and Vinayak S. Mane, "Phytochemical screening and Antibacterial Activity of Western Region wild leaf Colocasia esculenta," International Research Journal of Biological Sciences, 2013, Vol. 2(10), pp. 18-21.
3. Odedeji J. O., Oyeleke G. O., Ayinde L. A. and Azeez L. A., "Nutritional, Antinutritional Compositions and Organoleptic Analyses of Raw and Blanched Cocoyam (Colocasia esculenta) Leaves," IOSR Journal of Environmental Science, Toxicology and Food Technology, 2014, Vol. 8, Issue 2, pp 45-48.
4. Hedberg I, Hedberg O, Madat PJ, Mshigeni KE, Mshiu EN, Samuelsson G. Inventory of plants used in traditional medicine in Tanzania. II. Plants of the families Dilleniaceae—Opiliaceae. Journal of Ethnopharmacology. 1983 Nov 1; 9(1):105-27.
5. Kanbarkar N, Mishra S, Khanal P. Beneficial effect of phospholipase A2 group IIA inhibitors from Acacia suma in obesity: an in silico and in vitro study. Advances in traditional medicine. 2020 Dec 20:599-608.
6. Borhani DW, Shaw DE. The future of molecular dynamics simulations in drug discovery, J Comp Aid Mol 26: 15-26; 2012.
7. J. B. Harborne. Phytochemical Methods A GUIDE TO MODERN TECHNIQUES OF PLANT ANALYSIS Second Edition; 1984; 6-7.
8. Sarath P and Sudha Bai R. A comparative evaluation of phytochemicals in bark, leaves and seeds of *Putranjiva roxburghii* Wall. (Putranjivaceae). Journal of Pharmacognosy and Phytochemistry 2019; 8(1): 1162-1166.
9. Maurya S, Singh D, Quantitative Analysis of Total Phenolic Content in Adhatoda vasica Nees Extracts. Int J of Pharm Tech Res .2010; 2:2403-6.
10. Atanassova M, Georgieva S, Ivancheva K. Total phenolic and total flavonoid contents, antioxidant capacity and biological contaminants in medicinal herbs. Journal of the University of Chemical Technology & Metallurgy. 2011 Mar 1; 46(1).
11. C.L. Chang, C.S. Lin, G.H. Lai, Phytochemical characteristics, free radical scavenging activities, and neuroprotection of five medicinal plant extracts, Evid Based Compl. Altern. Med. 2012 (2012) 984295.
12. Stalons D.R., Thornsberry C. Broth-Dilution Method for Determining the Antibiotic Susceptibility of Anaerobic Bacteria. Antimicrob Agents Chemother, 7(1): 15–21, 1975.
13. Drew W.L., Barry A.L., O'Toole R., Sherris J.C. Reliability of the Kirby-Bauer disc diffusion method for detecting methicillin-resistant strains of Staphylococcus aureus. Appl Microbiol, 24(2): 240–247, 1972.
14. Ruch R.J., Cheng S.J. & Klaunig J.E. Prevention of cytotoxicity and inhibition of Intracellular communication by antioxidant catechins isolated from Chinese green tea. Carcinogenesis. 1989; 10: 1003–1008.
15. Siwe-Noundou X, Musyoka TM, Moses V, Ndinteh DT, Mnkandhla D, Hoppe H, Tastan Bishop Ö, Krause RW. Anti-HIV-1 integrase potency of methylgallate from Alchornea cordifolia using in vitro and in silico approaches. Scientific reports. 2019 Mar 18; 9(1):4718.
16. Deepak Kumar . M. Poornima . R. N. Kushwaha . Tae-Jin Won . Chuljin Ahn . C. Ganesh Kumar . Kiwan Jang . Dong-Soo Shin. Antimicrobial and docking studies of (2)-catechin derivatives. J Korean Soc Appl Biol Chem (2015) 58(4):581–585.
17. Ragunathan A, Ravi L. Potential antibacterial drug targets for quercetin and rutin: An in silico study using AutoDock. Der Pharmacia Lettre. 2015; 7(11):68-72.
18. Kim BG, Sung SH, Jung NR, Chong Y, Ahn JH. Biological synthesis of isorhamnetin 3-O-glucoside using engineered glucosyltransferase. Journal of Molecular Catalysis B: Enzymatic. 2010 May 1; 63(3-4):194-9.
19. Al-Nour MY, Ibrahim MM, Elsaman T. Ellagic acid, Kaempferol, and Quercetin from Acacia nilotica: Promising combined drug with multiple mechanisms of action. Current pharmacology reports. 2019 Aug 15; 5(4):255-80.
20. Pitaloka DA, Ramadhan DS, Arfan, Chaidir L, Fakih TM. Docking-based virtual screening and molecular dynamics simulations of quercetin analogs as enoyl-acyl carrier protein reductase (InhA) inhibitors of Mycobacterium tuberculosis. Scientia Pharmaceutica. 2021 May 20; 89(2):20.
21. Evangelina IA, Herdiyati Y, Laviana A, Rikmasari R, Zubaedah C, Anisah, Kurnia D. Bio-Mechanism inhibitory prediction of β-sitosterol from Kemangi (Ocimum basilicum L.) as an inhibitor of MurA enzyme of oral bacteria: In vitro and in silico Study. Advances and Applications in Bioinformatics and Chemistry. 2021 Jun 23:103-15.

22. Uttu AJ, Sallau MS, Ibrahim H, Iyun OR. Isolation, characterization, and docking studies of campesterol and β-sitosterol from Strychnos innocua (Delile) root bark. Journal of Taibah University Medical Sciences. 2023 Jun 1; 18(3):566-78.

23. Kullappan M, Benedict BA, Rajajagadeesan A, Baskaran P, Periadurai ND, Ambrose JM, Gandhamaneni SH, Nakkella AK, Agarwal A, Veeraraghavan VP, Surapaneni KM. Ellagic acid as a potential inhibitor against the nonstructural protein NS3 helicase of Zika virus: A molecular modelling study. BioMed Research International. 2022 Aug 21; 2022.

24. Refwalu MH, Indrayati A, Purwidyaningrum I. Studi Literatur Mekanisme Molekuler Antibakteri dari Daun Telang (Clitoria ternatea L.) Literature Study of Molecular Antibacterial Mechanism of Butterfly Pea (Clitoria ternatea L.) Leaves. Vol 20 No 1 (2023): Jurnal Farmasi Indonesia.

25. Malau ND, Azzahra SF. Analysis docking of plasmodium falciparum enoyl acyl carrier protein reductase (pfenr) with organic compunds from virtual screening of herbal database. Journal of Applied Chemical Science. 2018; 5(2):491-6.

26. SwissADME: a free web tool to evaluate pharmacokinetics, drug-likeness and medicinal chemistry friendliness of small molecules. Sci. Rep. (2017) 7:42717.

27. López-Blanco JR, Aliaga JI, Quintana-Ortí ES and Chacón P. (2014) iMODS: Internal coordinates normal mode analysis server. Nucleic acids research. Epub 2014 Apr 25; 42:W271-6.